

Development of electrical activity in cardiac myocyte aggregates derived from mouse embryonic stem cells

K. Banach,¹ M. D. Halbach,¹ P. Hu,¹ J. Hescheler,¹ and U. Egert²

¹Institut für Neurophysiologie, Universität zu Köln, 50931 Köln; and ²Institut für Neurobiologie und Biophysik, Institut für Biologie III, Albert-Ludwigs Universität Freiburg, 79104 Freiburg, Germany

Submitted 19 December 2001; accepted in final form 3 February 2003

Banach, K., M. D. Halbach, P. Hu, J. Hescheler, and U. Egert. Development of electrical activity in cardiac myocyte aggregates derived from mouse embryonic stem cells. *Am J Physiol Heart Circ Physiol* 284: H2114–H2123, 2003. First published February 6, 2003; 10.1152/ajpheart.01106.2001.—Embryonic stem cells differentiate into cardiac myocytes, repeating in vitro the structural and molecular changes associated with cardiac development. Currently, it is not clear whether the electrophysiological properties of the multicellular cardiac structure follow cardiac maturation as well. In long-term recordings of extracellular field potentials with microelectrode arrays consisting of 60 substrate-integrated electrodes, we examined the electrophysiological properties during the ongoing differentiation process. The beating frequency of the growing preparations increased from 1 to 5 Hz concomitant to a decrease of the action potential duration and action potential rise time. A developmental increase of the conduction velocity could be attributed to an increased expression of connexin43 gap junction channels. Whereas isoprenaline elicited a positive chronotropic response from the first day of spontaneous beating onward, a concentration-dependent negative chronotropic effect of carbachol only developed after ~4 days. The in vitro development of the three-dimensional cardiac preparation thus closely follows the development described for the mouse embryonic heart, making it an ideal model to monitor the differentiation of electrical activity in embryonic cardiomyocytes.

cardiac development; microelectrode array; excitation spread; connexin43; mouse embryonic stem cells

EMBRYONIC STEM (ES) cells differentiate in vitro into various cell types including cardiac myocytes (7). Previous studies on this system have shown that ES cell-derived cardiac myocytes (ESCs) express cardiac-specific proteins including α -actinin and α -myosin heavy chain in a time-dependent manner. The cell morphology gradually changes from a small and round shape to larger rod-shaped cells with recognizable myofibrillar assemblies (13, 15, 28, 37). Furthermore, electrophysiological measurements on isolated ESCs demonstrate a time-dependent expression of ion channels and signal transduction pathways (1, 12, 24, 25). The differentiation of the ESCs in culture therefore seems to recapitulate steps of the in vivo embryonic differentiation of cardiac muscle. Action potential (AP) recordings on

isolated ESCs suggest that these cells differentiate into specific cardiac cells such as atrial, ventricular, and pacemaker cells (15, 25). Although their distribution within the beating aggregate of ESCs has not been completely analyzed, in vivo stainings and tissue-specific expression of green fluorescent protein indicate that different cellular phenotypes are arranged in aggregates rather than randomly distributed (27, 28). However, it is currently not clear how the developmental and tissue-specific differentiation relates to the electrophysiological properties of the intact three-dimensional preparation of ESCs. In the present study, we analyzed the developmental changes of spontaneous electrical activity with repeated multielectrode recordings using substrate-integrated microelectrode arrays (MEAs). This technique allows not only the long-term culture of the preparation but also the analysis of the spatial electrophysiological differences within the preparation. In the present study, we analyzed different field potential (FP) parameters to characterize the development of the spontaneous electrical activity of multicellular aggregates of ESCs and their electrophysiological properties. Furthermore, the use of an ES cell line deficient in the expression of connexin43 (Cx43^{-/-}), the major cardiac gap junction protein, enabled us to distinguish developmental changes of the active, voltage-dependent membrane properties from changing passive components like the intercellular resistance.

MATERIALS AND METHODS

Culture of ES cells. ES cells of the cell lines D3 and R1 [Cx43^{-/-} (31, 34)] were propagated in culture and differentiated within three-dimensional embryo-like structures called embryoid bodies (EBs) as described previously (16, 25). Briefly, ES cells were propagated on feeder cell layers with leukemia-inhibiting factor (LIF) added to the culture medium. Differentiation was initiated by the “hanging drop” method (400 cells/20- μ l drop) and withdrawal of LIF. After 2 days, the drops were washed off the lid of the culture dish, and EBs were maintained in suspension [DMEM plus supplements (46)] for another 5 days. After these 7 days, EBs were plated onto MEAs, which served as the FP recording device and culture dish at the same time. The EBs attached to the bottom of the MEA within 1 day after being plated (*day*

Address for reprint requests and other correspondence: K. Banach, Dept. of Physiology, Loyola Univ. Chicago, 2160 S. First Ave., Maywood, IL 60153 (E-mail: kbanac1@lumc.edu).

The costs of publication of this article were defrayed in part by the payment of page charges. The article must therefore be hereby marked “advertisement” in accordance with 18 U.S.C. Section 1734 solely to indicate this fact.

7+1) and subsequently spread to form a three-dimensional cell layer containing various cell types including cardiac myocytes (16, 46).

MEA recording. We used substrate-integrated, planar MEAs (Multi Channel Systems; Reutlingen, Germany) for long-term recordings of the spontaneous electrical activity from cultures of cardiac myocytes and EBs (8, 16). EBs were positioned in the middle of a sterilized MEA consisting of 60 titanium nitride-coated gold electrodes (diameter = 30 μm ; interelectrode distance 200 μm in a square grid). For recording, a separate sterile Ag/AgCl electrode was temporarily inserted into the dish as the ground electrode. The MEA was connected to the amplifier and data-acquisition system (Multi Channel Systems), which included a heating device to maintain a constant temperature of 37°C. Data were recorded simultaneously from up to 60 channels (sampling frequency up to 40 kHz) under sterile conditions. The data were analyzed off-line with a customized toolbox programmed for MATLAB (Mathworks; Natick, MA) to detect FPs. Figure 1A shows an example of voltage traces recorded from a small EB at *day 7+4* in culture. Electrical activity is reflected in the negative deflections of the voltage traces. In the magnification of the FP recorded from *electrode 56* (Fig. 1A, *left*), the FP parameters analyzed are depicted: the interspike intervals (ISI), the size of the largest negative peak (FP_{Min}), the last positive peak in a cycle (FP_{Max}), the duration of the FP (FP_{dur} ; defined as the interval between FP_{Min} and FP_{Max}), and the FP descent phase [FP_{rise} ; defined as the time from the onset of the FP (baseline) to FP_{Min}].

These parameter were chosen according to previous analysis and interpretations of FPs by Regeher et al. (36), Spach et al. (39), and Yamamoto et al. (47), who directly correlated

FP parameters to simultaneously recorded APs. After these interpretations, the decay of the extracellular waveform (here, FP_{rise}) is proportional to the duration of the upstroke of the intracellular potential (39). Furthermore, according to the data published by Yamamoto et al. (47), the slow return of the FP to the baseline coincides with the repolarization of the APs. We found, however, that the interval from FP_{Min} to FP_{Max} was a more reliable, relative correlate of the AP duration (FP_{dur}). Even though this analysis does not allow us a quantitative analysis of the currents contributing to the APs, changes in the parameters can be interpreted as changes in the contribution of different ion channels to the FP. The ISI represents the beating frequency of the preparation and could be measured for extended periods. Figure 1B shows the FP recorded from one MEA electrode over the period of 2 min. The ISI measured from this electrode is shown in Fig. 1C and revealed an ISI of 859.5 ± 39.9 ms (mean \pm SE). To control the validity of this measurement, usually the ISI at different electrodes within one preparation was analyzed and compared.

RESULTS

Development of spontaneous pacemaker activity in ES cells. ES cells differentiate *in vitro* into cardiac myocytes, thereby expressing cardiac-specific proteins in a time-dependent manner. By plating EBs on the MEA, we examined when electrical activity can be recorded from spontaneously beating cardiac myocytes and whether developmental changes of the electrophysiological properties can be quantified during the

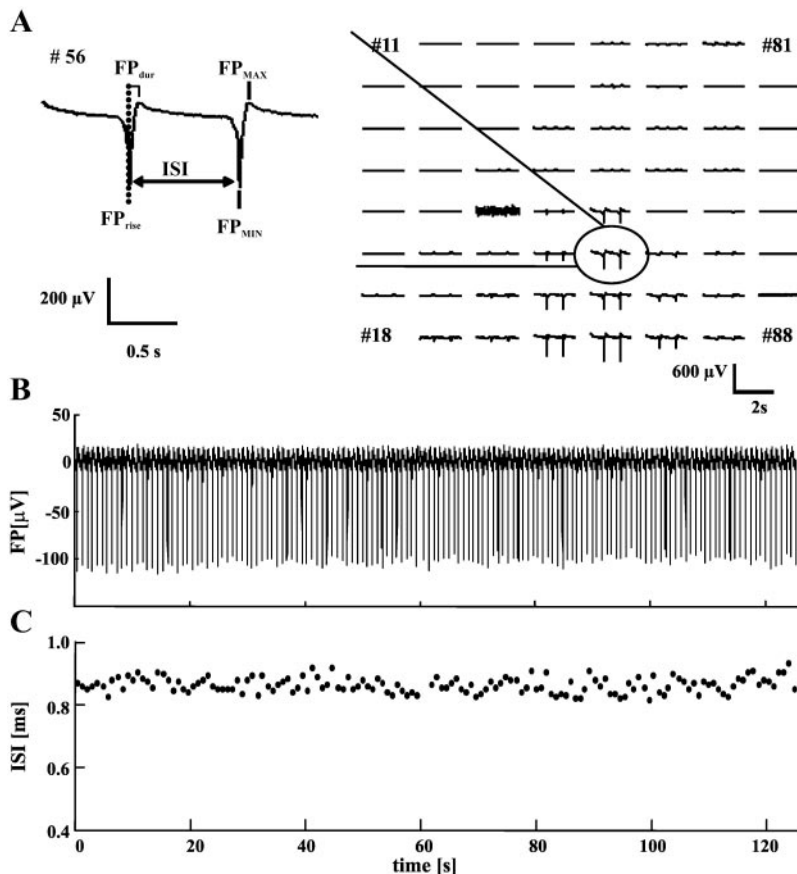


Fig. 1. A: field potentials (FPs) recorded from an embryonic body (EB) with a microelectrode array (MEA). The 8×8 arrangement of the traces reflects the arrangement of the electrodes. The parameters analyzed are indicated for the magnified FP. The interspike interval (ISI; C) was recorded from continuous FP recordings (B) on single MEA electrodes and is a reliable measure of the beating frequency (ISI = 859.5 ± 39.9 ms, mean \pm SE). FP_{Min} , size of the largest negative peak; FP_{Max} , last positive peak in a cycle; FP_{dur} , duration of the FP; FP_{rise} , FP descent phase.

developmental process. One or two days after being plated (i.e., *days 7+1* and *7+2*), cardiac cells were identified within beating aggregates of EBs. The development of visible beating coincided with the occurrence of negative deflections in the FPs recorded with the MEA. Figure 2A illustrates FPs recorded from the same EB preparation on subsequent days. Counting the number of electrodes with electrical activity gives us a relative measure for the size of the beating area and most likely reflects the growth of the cluster of electrically active cardiac cells (Fig. 2B; means \pm SE, $n = 21$ EBs). The number of active electrodes increased almost sevenfold during the first 10 days of culture. Concurrently, the amplitude of FP_{Min} increased. Although the degree of this change varied between electrodes within the beating area, the overall increase of FP_{Min} was reproducible. The increase of the beating area as well as the increase of FP_{Min} most likely indicates the developmental increase in the number of electrically active cardiac cells.

In addition, there was a clear developmental change of the spontaneous beating frequency of the ESC clusters. The ISI decreased with the age of the culture to ~ 0.2 s around *day 7 + 10* (Fig. 2C). The reproducibility of these findings in different EB preparations indicates

that this change of the ISI was not random but reflects a stable differentiation process.

Developmental change of the shape of the FP. During cardiac development of embryonic mice, the electrophysiological properties of the cells, like the AP upstroke velocity and AP duration, undergo significant changes (5, 41). To examine whether the developmental changes of the AP are reflected in changes of the FP during developmental differentiation within a beating aggregate of ESCs, we examined the waveform of FPs recorded from the same preparation on successive days. On the first day of spontaneous activity, FPs were small in amplitude and FP_{rise} was long; a representative example is shown in Fig. 3A. FPs throughout the aggregate exhibited a high degree of similarity at this state of development; however, in later stages, a temporal as well as developmental change could be observed. The average of all FPs within single preparations reveals an overall decrease of FP_{rise} up to *day 7+9* of development (Fig. 3B; means \pm SE, $n = 13$ EBs). However, during this period, the FPs within a single preparation grew more heterogeneous. Examining FP_{rise} along the path of excitation spread revealed that in ESCs FP_{rise} was long at the origin of excitation and shortened significantly with increasing distance from the pacemaker region (Fig. 3C).

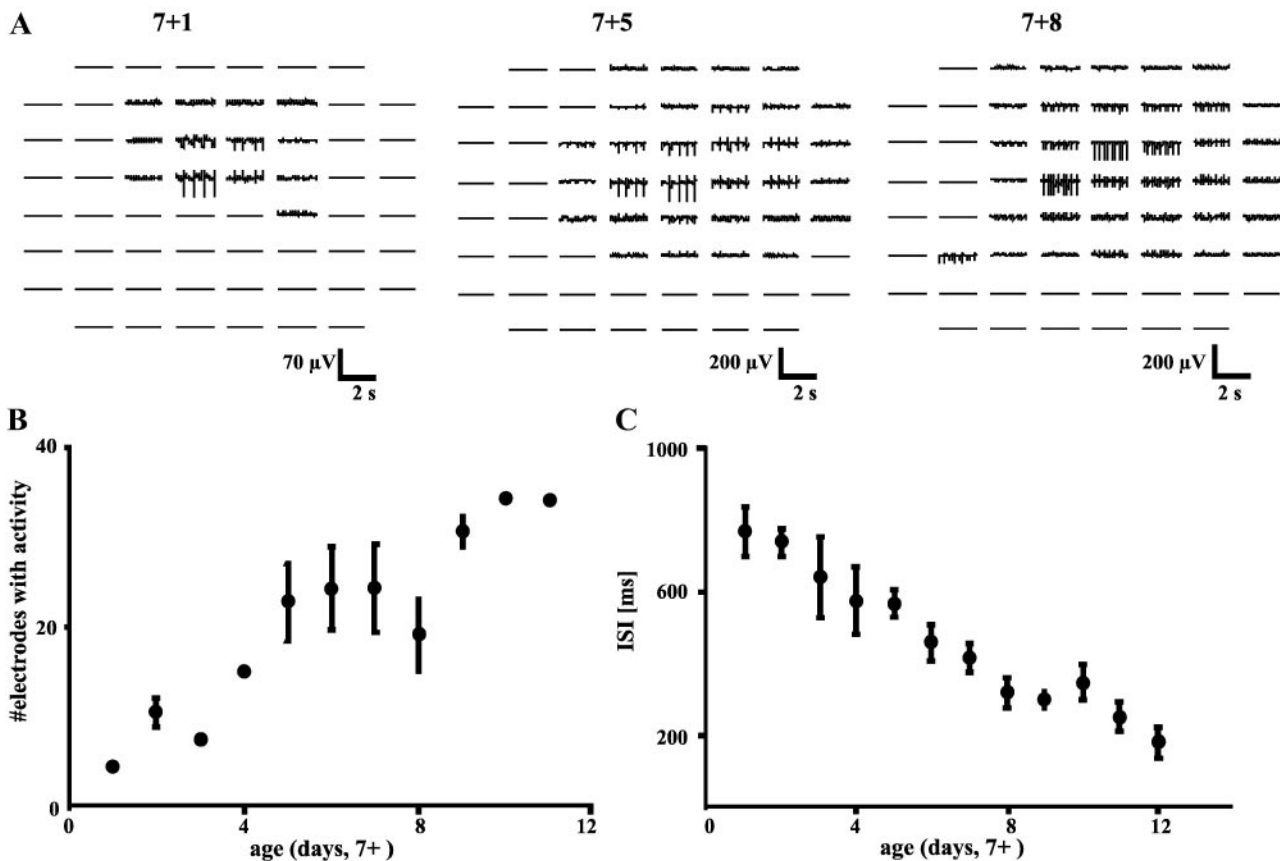


Fig. 2. A: FPs from one EB preparation recorded on *days 7+1*, *7+5*, and *7+8* of culture. Traces from positions without detectable activity were omitted (lines indicate 0- μ V level only). The number of electrodes and FP_{Min} increased during development. B: the number of electrodes with electrical activity increased sevenfold during the first 10 days of culture (means \pm SE, $n = 21$). C: in the same period, the ISI (means \pm SE, $n = 19$) decreased.

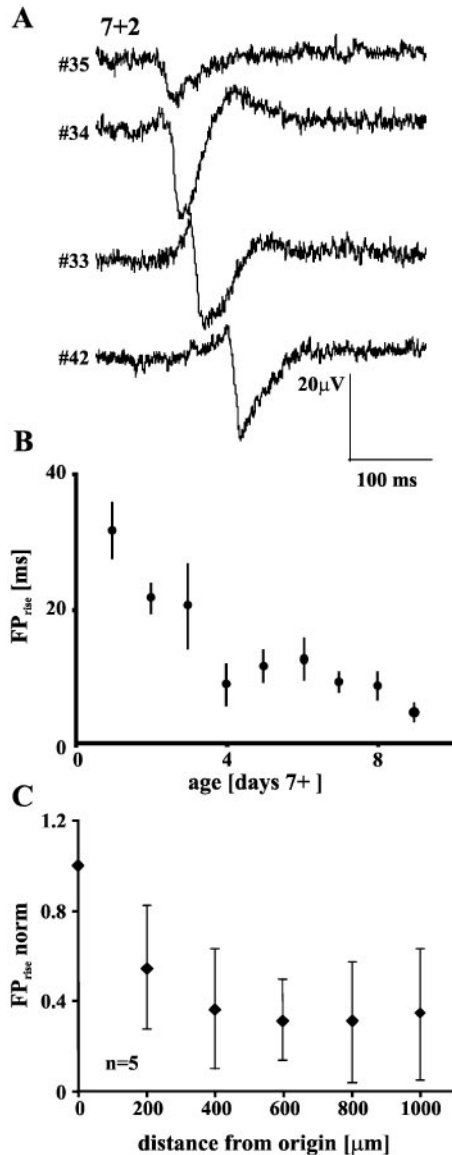


Fig. 3. FPs (A) recorded simultaneously on *day 7+2* of development on *electrodes 35, 34, 33, and 42*. The succession of FP_{Min} indicates the delay of excitation spread. *B*: FP_{rise} (means \pm SE, $n = 10$ EBs) plotted versus time in culture. *C*: normalized FP_{rise} as a function of the distance from the origin of excitation (means \pm SE, $n = 5$).

Taking the data of Yamamoto et al. (47) as a basis that the repolarization of the AP coincides with the return of the negative potential to the baseline, we were able to characterize the developmental changes of AP duration in ESCs. To assess the overall development of FP_{dur} on successive days of development, we averaged the FP_{dur} over all active electrodes for each preparation and found a developmental decrease that stabilized around *day 7+10* (Fig. 4A; $n = 19$ EBs). To demonstrate that FP_{dur} also follows experimentally induced changes of the AP duration, we exposed ESCs to increasing concentrations of 4-aminopyridine (4-AP), a blocker of the transient outward K^+ current (I_{to}) known to prolong AP duration in mouse ventricular cells (32, 43) and ESCs (12). A concentration-depen-

dent increase of FP_{dur} could be observed (Fig. 4C), concomitantly with a decrease of the ISI (Fig. 4B).

Developmental change of the propagation velocity. The MEA system enables us to determine the origin and direction of excitation spread from the temporal succession of FP_{Min} (16) on the surrounding electrodes. In Fig. 5A, the delay of excitation spread recorded from a single preparation at *days 7+2* and *7+5* of culture is plotted against the respective distance of the electrodes from the origin of excitation. At the onset of beating

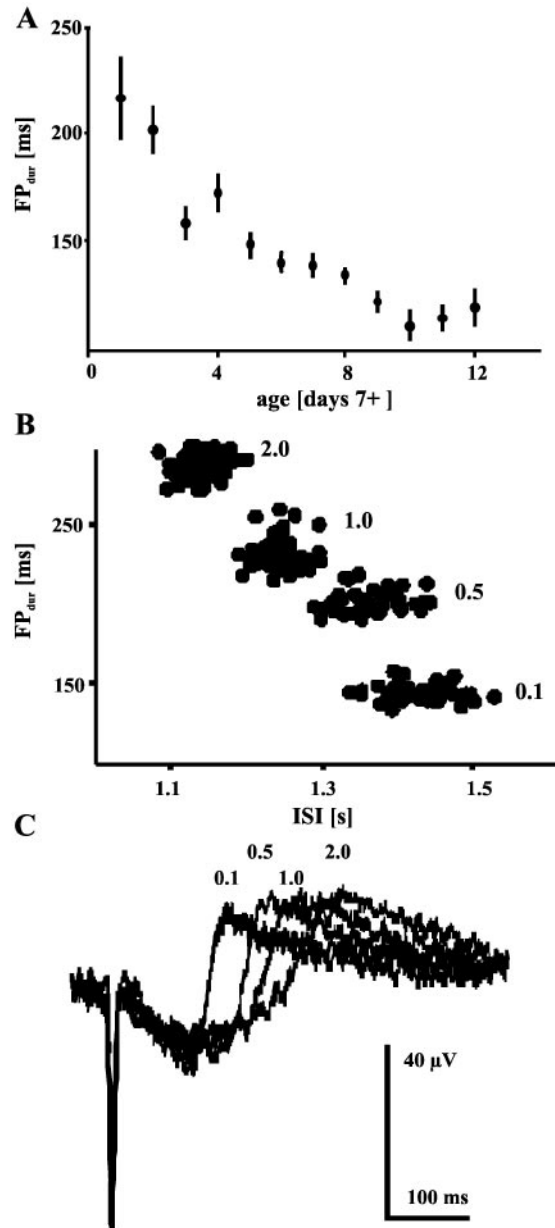


Fig. 4. *A*: FP_{dur} plotted as a function of time in culture (means \pm SE, $n = 19$ EBs). FP_{dur} estimated from FPs from the experiment illustrated in *C* are plotted versus ISI (*B*). Numbers indicate the concentrations of 4-aminopyridine (4-AP; in mmol/l) in the bath. Each cluster represents FPs recorded during a time period of 30 s. Note that the ISI shortened, although the action potential lengthened, with increasing concentrations. *C*: representative voltage traces of FPs recorded at the 4-AP concentrations indicated.

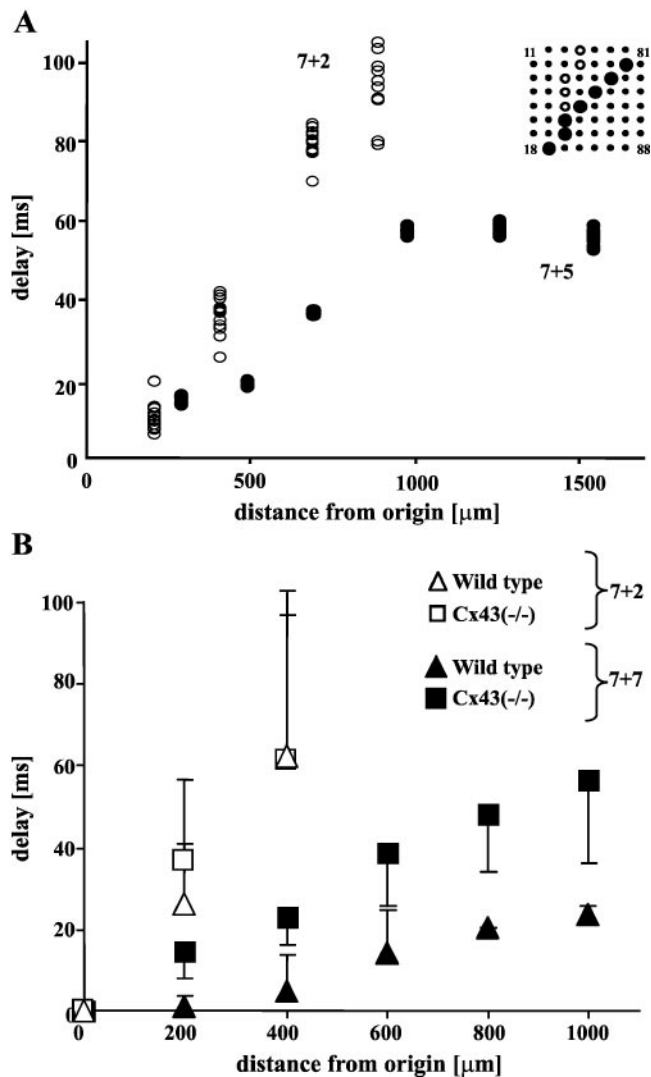


Fig. 5. The delay of excitation spread decreased during time in culture. *A*: path of excitation spread in 7+2 (\circ)- and 7+5 (\bullet)-day-old EB preparations. In both cases, excitation started at the lowermost electrode. Plotting the delay of each electrode versus its distance from the origin of excitation reveals a significant decrease in the delay of excitation spread during time in culture. *B*: delay of excitation spread in 7+2 (\circ)- and 7+7 (\bullet)-day-old embryonic stem cell-derived cardiac myocytes (ESCs) derived from wild-type and connexin43-deficient (Cx43^{-/-}) preparations. (Four different EB preparations from each cell line at both developmental stages were included in the analysis.)

(day 7+2), a delay of almost 30 ms for a 200- μm distance can be observed, corresponding to a conduction velocity of 6×10^{-3} m/s. Examination of the same preparation at day 7+5 in culture reveals an increase of the beating area and an increase of the velocity of excitation spread. The path of excitation spread is again marked on the sketch of the MEA (open circles, Fig. 5A). Plotting the interelectrode delay against the distance from the origin of excitation, now located at the bottom left end of the MEA, reveals that the delay is markedly decreased, reflecting a conduction velocity of $\sim 15 \times 10^{-3}$ m/s. Calculating absolute propagation velocities requires detailed information about the exact

path of excitation propagation within the cell syncytium of the EB. Because information about these parameters is not readily available in this preparation, the values can only be taken as approximations. The increase of the conduction velocity could be based on a developmental increase in the current density of fast-activating voltage-dependent channels, increased expression of gap junction channels (2, 40), increased tissue organization, or an increase in cellular size. To rule out that the increase is solely due to the structural features of the preparation, we studied the developmental change of the conduction velocity in preparations of ESCs lacking the expression of Cx43, the major cardiac gap junction protein whose expression is up-regulated in the cardiac tissue at embryonic day 9.5 postcoitum (E9.5) (2). Cardiomyocyte aggregates derived from Cx43^{-/-} cells exhibited the same time-dependent change of ISI, FP_{rise}, and FP_{dur} as observed in wild-type cells. In contrast, differences in the developmental change of the conduction velocity could be observed. At the onset of beating at day 7+1/7+2 (open symbols, Fig. 5B), both cell lines exhibited similar low conduction velocities (6×10^{-3} m/s), although the developmental increase of the conduction velocity in cultures older than 7+7 days (open symbols, Fig. 5B) was significantly higher in the wild-type than in the Cx43^{-/-} cell line. Whereas conduction velocities of $\sim 15 \times 10^{-3}$ m/s were reached in the Cx43^{-/-} preparation, wild-type preparations reached an average of 45×10^{-3} m/s. This observation suggests that the developmental expression of Cx43 underlies the structural maturation of the tissue and is responsible for the developmental increase in conduction velocity.

Development of hormonal sensitivity. The responsiveness of the early murine embryonic heart to β -adrenergic stimulation is controversial in the literature. Whereas some reports describe that the positive chronotropic and inotropic responses to β -adrenergic stimulation lag behind the expression of β -adrenergic receptors (3, 4), the newer studies of Liu et al. (22) describe positive chronotropic effects on whole hearts as well as on single cardiac myocytes of 9-day-old mouse embryos. The negative chronotropic effect in the heart is mediated by carbachol (CCh) via the activation of muscarinic K⁺ current ($I_{K,ACh}$). In chicken as well as rat hearts, a negative chronotropic response to CCh develops only later in development. To test whether the susceptibility of the pacemaker to adrenergic and cholinergic stimulation in ESCs repeated this change during the differentiation process in culture, we perfused the cells at different stages of development with either the β -receptor activator isoprenaline (Fig. 6) or CCh (Fig. 7). Already at the first day of spontaneous electrical activity (in this preparation, day 7+2), we observed a positive chronotropic effect of β -receptor stimulation ($n = 3$; Fig. 6A). Application of CCh induced a concentration-dependent negative chronotropic effect only around day 7+5 (Fig. 7A) of development ($n = 3$ for preparations older than 7+5 days and $n = 4$ for preparations younger than 7+5 days). A transient and a steady-state component can be distin-

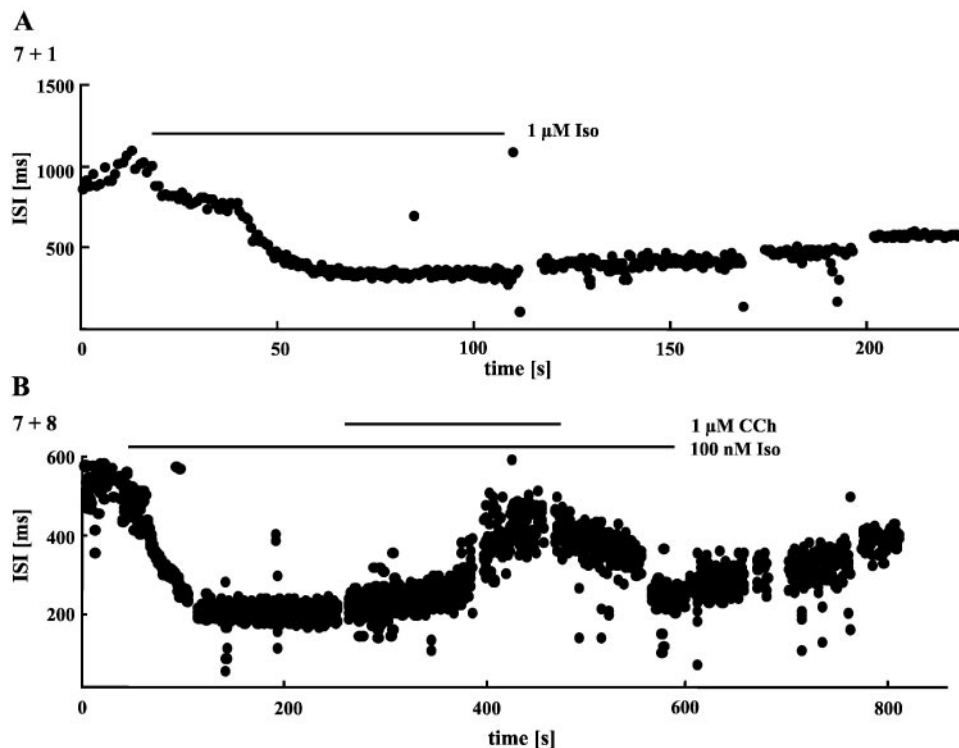


Fig. 6. ISI plotted against the time of recording. *A*: isoprenaline (Iso) induced a decrease of ISI in a preparation that started beating at *day 7+2* of culture. *B*: at *day 7+8*, carbochol (CCh; 1 μ M) antagonized reversibly the positive chronotropic effect induced by Iso (100 nM).

guished in the frequency response. The sensitivity of the culture toward CCh increased during subsequent days of development (Fig. 7*B*). In the same culture, identical concentrations of CCh (10 and 50 μ M) now induced a transient block of pacemaker activity before

beating resumed at a decreased steady-state frequency (Fig. 7*B*). The antagonizing effect of CCh on β -adrenergic stimulation was likewise only detected in older cultures. Application of isoprenaline to a preparation at *day 7+8* in culture induced a decrease of the ISI from

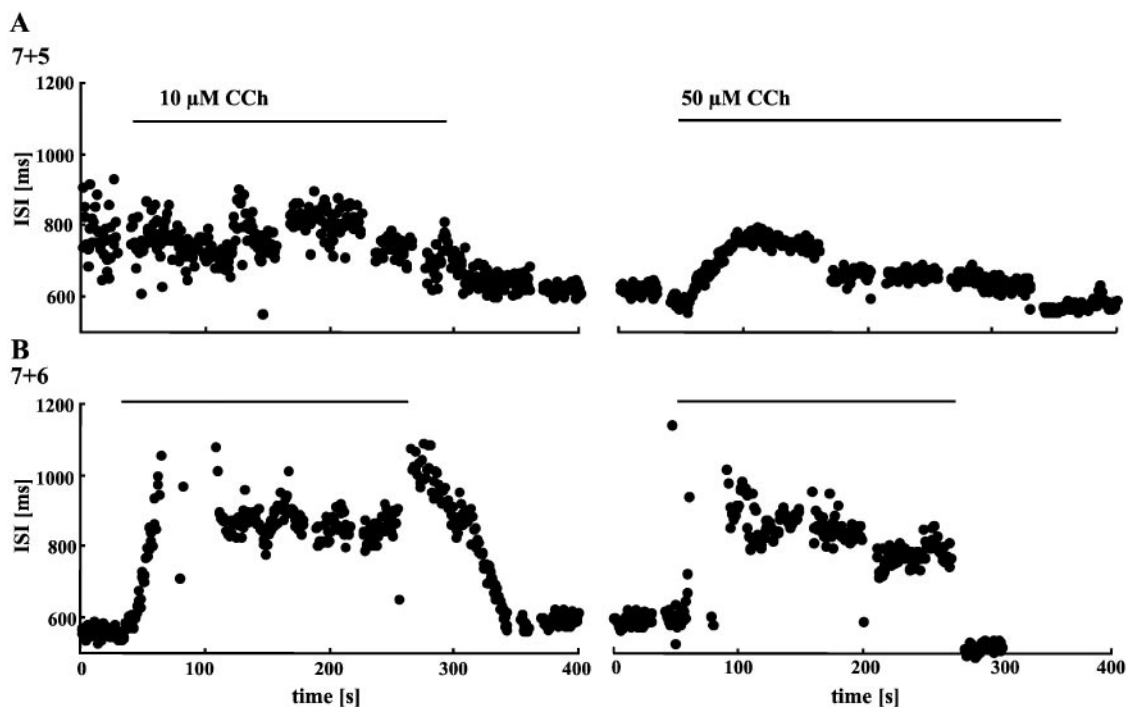


Fig. 7. *A*: at *day 7+5*, the negative chronotropic effect of CCh is reflected in a small increase of the ISI. Only 1 day later (*B*; *day 7+6*), the same preparation responded to the identical concentration of CCh with a transient block of the spontaneous activity and a more pronounced increase in the steady-state ISI.

500 to 200 ms (Fig. 6B). Additional transient perfusion with CCh resulted in a reversible decrease of the beating frequency. The experiments demonstrate that ESCs not only change their spontaneous electrical activity in culture but also that their sensitivity to hormonal stimuli changes during the differentiation process.

DISCUSSION

Previous characterizations of the developmental steps associated with segregation of electrically and functionally different cell types in the developing heart relied on either whole organ preparations (19, 20) or the isolation of single cells from the embryonic heart (32, 43, 44). With both techniques, electrophysiological properties at the stage of organ isolation can be described, but continuous measurement of the differentiation process is limited. Furthermore, culture conditions are known to initiate remodeling of isolated cells (9, 14). Mouse as well as human ES cells, on the other hand, are known to recapitulate molecular stages of the developmental process of cardiac myocytes (21, 28, 37, 45), and electrophysiological and intrinsic properties of the APs could be described in single-cell cardiac myocyte preparations (1, 12, 23).

We report here for the first time how the sequence of change of the electrophysiological properties and its interplay with the structural change of the multicellular cardiac preparation result in the spontaneous electrical activity recorded in a multicellular *in vitro* model of cardiac development. With the differentiating EBs plated on a MEA, we were able to continuously monitor the spatial and temporal structure and the dynamics of electrical activity of a developing multicellular structure of cardiac myocytes. Besides the analysis of the beating frequency and the velocity of excitation spread by means of the FP, we analyzed developmental changes of FP parameters that are proportionally related to the duration of the AP upstroke (39) and AP duration (47). With the repeated, comparative analysis of these parameters within the same specimen of wild-type and genetically manipulated preparations, the importance of individual components for the developmental or pathophysiological change of spontaneous electrophysiological properties can be revealed.

Comparison of FPs recorded from ESCs and isolated cardiac myocytes. In differentiating EBs, cells of all three germ layers can be detected (7), although the distribution of different cell types inside an EB needs to be analyzed in detail. Oyamada et al. (33) reported that no dye coupling takes place between cardiac and noncardiac cells in the EB, indicating that cardiac cells are electrically isolated from the surrounding tissue. Because electrical coupling could influence the shape of the FPs recorded at electrodes not in direct contact with electrically active cells, we compared FPs recorded from ESCs and, presumably more homogeneous, monolayers of cardiac myocytes isolated from the embryonic mouse heart (K. Banach, unpublished data). Although the structure of ESCs is more complex,

the recordings revealed no qualitative or quantitative differences of the waveforms. The FP types recorded in cardiac myocyte cultures were also found in EB recordings, suggesting that the same mechanisms generate these fields and that the same currents likely form their basis.

Developmental change of the FP in ESCs. The average number of electrodes detecting electrical activity in recordings from differentiating ESCs increased sevenfold during the first 10 days of culture. An increase in the surface of the beating aggregate due to the increase in cell size or migration of cells from the EB as described for this preparation (46) cannot be ruled out; however, previous studies report the withdrawal of ESCs from the cell cycle only at *day 16 (day 7+9)* (26) and increasing cardiomyocyte numbers until *day 7+14* of differentiation (30). Therefore, at least during the first 10 days after the cells were plated, the mitotic activity seems to play a significant role in the increase of the beating aggregate. During the increase of the beating aggregate, the beating frequency increased from initially 1 to 5 Hz. The time course of the functional development of the cardiomyocyte structure within the EB compares well with that of the developing embryonic mouse heart (35), where electrical as well as contractile activity start at 8.5 days postcoitum, when myocardium is still added to the heart tube (10, 29, 30).

The electrophysiological basis of the increased beating frequency could depend on multiple factors. In isolated ESCs, intracellular Ca^{2+} oscillations as well as ATP-dependent K^+ channels, I_{to} , and the pacemaker current (I_{f}) have been described to play an important role in the development of pacemaker activity (1, 12). The developmental increase in frequency therefore could be based on either a switch between the major mechanisms of pacemaker activity or an increased current density of the responsible current component as described for I_{f} in ESCs (1).

Besides an increase of the beating frequency, we observed within the area of differentiating cardiac myocytes 1) an increase of FP_{rise} , 2) a decrease of FP_{dur} , and 3) an increase of the propagation velocity. These parameters relate to the following changes of the intrinsic electrophysiological properties described for isolated ESCs and cardiac cells isolated from embryonic mice.

First, all FPs recorded at the time of onset of visible beating, i.e., *days 7+1* or *7+2*, exhibited a homogenous shape with a long FP_{rise} and prolonged FP_{dur} (Figs. 3A and 4, A and B). This result corresponds to the slow rise times described for APs recorded from the embryonic chicken (11, 19, 20) and from isolated ESCs up to *day 7+3* in culture (24). The potentials were similar to those recorded from the origin of excitation in EBs at later stages of development (Fig. 3C). These data indicate that all cells are functionally homogeneous and pacemaker-like at the onset of beating and that no fast voltage-activated depolarizing currents like Na^+ current are involved in the generation of the AP, consistent with the findings in isolated ESCs (24). As a

caveat, it must be noted that FP_{Min} also depends on the absolute current flowing at the location of an electrode. This is influenced by the increasing number of electrically coupled cells and their intercellular resistance within the range of the MEA electrode, which, in turn, is suggested by the growth of the EB described above. It is important to note that pacemaker-like FPs with long descent times found at the origin of excitation spread within the multicellular aggregate (Fig. 3C) did not necessarily produce the smallest FP_{Min} values within a culture, as would be expected for small, weakly coupled populations. This supports the interpretation that the decrease of FP_{rise} reflects the development of fast depolarizing currents.

Second, the developmental decrease of the AP duration points out the ongoing differentiation process. In the mouse heart, a developmental decrease of the AP duration was attributed to complex changes of the expression level of different ion channels responsible for repolarization. The current density of I_{to} from the neonatal to adult heart, as well as the current density of the rapid and slow components of the delayed rectifier K^+ current, increases during embryonic development (5, 44) and during the developmental differentiation of ESCs (12). Up to now, we did not identify the current component responsible for the accelerated repolarization, but a developmentally increased expression of outward rectifying currents could be demonstrated in single ESCs isolated from beating aggregates (12). Additionally, the marked increase of FP_{dur} after application of 4-AP indicates the expression of I_{to} in our multicellular preparations and supports a shortening of the AP due to the differentiation of these K^+ currents.

Finally, in the ESCs derived from wild-type as well as $Cx43^{-/-}$ ES cells, a developmental increase in the conduction velocity could be observed, whereas the increase in the wild-type preparations exceeded that of the $Cx43^{-/-}$ cells by a factor of 3. Besides the increased density of fast voltage-activated channels, the propagation velocity inside a cardiac preparation depends on the intercellular resistance as well as the size and structural arrangement of the cells in the electrical syncytium (40). An increased density of the voltage-dependent Na^+ current was previously described during embryonic development (4) and in differentiating ESCs (25) and is in good agreement with the increased FP_{rise} observed in our FP measurements. However, because cardiac myocytes isolated from $Cx43^{-/-}$ mice exhibit similar densities of the voltage-dependent Na^+ current to those of wild-type cells (18), the increase in conduction velocity cannot completely be attributed to the increased AP rise time. The cellular structure of ESCs, which is similar to that of cardiac myocytes, develops from a small and round cell to a larger, rod-shaped cell with recognizable myofibrillar assemblies (13, 15, 45, 46). These changes could also be observed in our culture, although no differences between the wild-type and $Cx43^{-/-}$ preparations could be observed. The earliest gap junction channel protein expressed in the embryonic heart is $Cx45$, which is also ex-

pressed in ES cells (33, 45), forms a low-conductance channel that is believed to be the reason for the slow peristaltic contractions of the embryonic mouse heart (2). Expression of the cardiac gap junction proteins $Cx40$ and $Cx43$ follows at E9.5 of the embryonic mouse heart development (2). The expression of all three connexins is described for ES cells. Increased expression of $Cx40$ was found to coincide with the occurrence of cardiac myocytes (33), and $Cx43$ expression could be demonstrated within the ESCs by immunohistochemistry (33, 45). The structural reorganization of the cells in conjunction with an increased density of fast voltage-dependent ion channels (13, 25) might thus account for the developmental decrease in the conduction velocity of $Cx43^{-/-}$ and wild-type ESCs, although the further reduction in the wild-type cells might be attributed to the developmentally increased expression of $Cx43$.

Development of hormonal sensitivity. Besides the expression of voltage-dependent ion channels, electrical activity of cardiomyocytes depends crucially on their sensitivity to modulation by the vegetative or autonomous nervous system. We could demonstrate that adrenergic and cholinergic sensitivities are regulated differentially during the differentiation of ESCs in vitro. Whereas the positive chronotropic effect of isoprenaline is present from the onset of spontaneous beating activity (*day 7+2*), the negative chronotropic effect of CCh developed only around *day 7+4* of in vitro differentiation. Our data are thus in agreement with results obtained from the intact embryonic mouse heart, in which a positive inotropic effect of isoprenaline was observed on whole hearts and isolated ventricles of 9.5 days postculture, 1 day after the initiation of spontaneous beating (22). Only later in development does the negative chronotropic effect of CCh on embryonic heart start. Davies et al. (4) described the expression of $I_{K_{\text{ACh}}}$ only after 17 days postculture in mouse atrial cells. In the rat and chicken, the negative chronotropic effect of CCh is not established from the beginning of contractile activity (6, 42). However, in previous experiments on the sensitivity of ESCs for CCh and isoprenaline on isolated ESCs in the whole cell patch-clamp configuration, Maltsev et al. (23) described that L-type Ca^{2+} current was insensitive to isoprenaline, forskolin, and cAMP until *day 7+9* in culture. Furthermore, stimulation of I_f by isoprenaline could only be found in late-stage cells. In contrast, the inhibitory effect of CCh on I_f was already developed in early cells (1, 17). This contrast to our findings might be caused by the isolation procedure and the dedifferentiation of isolated cells in culture, which lack the influence of the surrounding noncardiac tissue in the EB. Another possibility is a spatially, in terms of their receptor expression, heterogeneous differentiation of the cells in the multicellular aggregate that cannot be distinguished after the isolation procedure.

In conclusion, in this study, we demonstrated that the developmental succession of the electrophysiological properties of multicellular preparations of ESCs matches the sequence of electrophysiological changes

described for the embryonic heart. The combination of the ES cell and the MEA technique not only allowed the characterization of the beating frequency and the propagation velocity during development, but also enabled the analysis of concurrent changes of intrinsic AP properties, such as AP rise time and AP duration. Additionally, the study on the differentiation of wild-type and Cx43^{-/-} ESCs revealed the electrophysiological and structural interplay during the development of pacemaker activity and excitation spread.

We thank Dr. J. Rossant for providing the Cx43^{-/-} cell line.

This research was supported by Bundesministerium für Bildung und Forschung Grants FKZ 0310967, 0310965, and 0310964D. K. Banach was funded by the Lise Meitner-Habilitationsstipendium of Nordrhein Westfalen.

REFERENCES

1. **Abi-Gerges N, Ji GJ, Lu ZJ, Fischmeister R, Hescheler J, and Fleischmann BK.** Functional expression and regulation of the hyperpolarization activated non-selective cation current in embryonic stem cell-derived cardiomyocytes. *J Physiol* 523: 377–389, 2000.
2. **Alcolea S, Theveniau-Ruissy M, Jarry-Guichard T, Marics I, Tzouanacou E, Chauvin JP, Briand JP, Moorman AFM, Lamers WH, and Gros DB.** Downregulation of Cx45 gene products during mouse heart development. *Circ Res* 84: 1365–1379, 1999.
3. **An RH, Davies MP, Doevendans PA, Kubalak WS, Bangalore R, Chien KR, and Kass RS.** Developmental changes in beta-adrenergic modulation of L-type Ca²⁺ channels in embryonic mouse heart. *Circ Res* 78: 371–378, 1996.
4. **Chen FC, Yamamura HI, and Roeske WR.** Adenylate cyclase and beta-adrenergic receptor development in the mouse heart. *J Pharmacol Exp Ther* 222: 7–13, 1992.
5. **Davies MP, An RH, Doevendans P, Kubalak S, Chien KR, and Kass RS.** Developmental changes in ionic channel activity in the embryonic murine heart. *Circ Res* 78: 15–25, 1996.
6. **Dong L, Sperelakis N, and Wahler GM.** Development of physiological responses to acetylcholine during organ culture of young embryonic chick hearts. *J Dev Physiol* 8: 307–314, 1986.
7. **Doetschman TC, Eistetter H, Katz M, Schmidt W, and Kemler R.** The in-vitro development of blastocyst-derived embryonic stem cell lines: formation of visceral yolk sac, blood islands and myocardium. *J Embryol Exp Morphol* 87: 27–45, 1985.
8. **Egert U, Schlosshauer B, Fennrich S, Nisch W, Fejtl M, Knott T, Mueller T, and Hämmerle H.** A novel organotypic long-term culture of the rat hippocampus on substrate-integrated multielectrode arrays. *Brain Res* 2: 229–242, 1998.
9. **Eppenberger M, Hauser I, and Eppenberger HM.** Myofibril formation in long term-cultures of adult rat heart cells. *Biomed Biochim Acta* 46: S640–S645, 1987.
10. **Fishman MC and Chien KR.** Fashioning the vertebrate heart: earliest embryonic decisions. *Development* 124: 2099–2117, 1997.
11. **Fuji S, Hirota A, and Kamino K.** Optical recording of development of electrical activity in embryonic chick heart during early phases of cardiogenesis. *J Physiol* 311: 147–160, 1981.
12. **Gryshchenko O, Lu ZJ, Fleischmann BK, and Hescheler J.** Outward currents in embryonic stem cell-derived cardiomyocytes. *Pflügers Arch* 439: 798–807, 2000.
13. **Guan K, Furst DO, and Wobus AM.** Modulation of sarcomere organization during embryonic stem cell-derived cardiomyocyte differentiation. *Eur J Cell Biol* 78: 813–823, 1999.
14. **Guo JX, Jacobson SL, and Brown DL.** Rearrangement of tubulin, actin, and myosin in cultured ventricular cardiomyocytes of the adult rat. *Cell Motil Cytoskeleton* 6: 291–304, 1986.
15. **Hescheler J, Fleischmann BK, Lentini S, Maltsev VA, Rohwedel J, Wobus AM, and Addicks K.** Embryonic stem cells: a model to study structural and functional properties in cardiomyogenesis. *Cardiovasc Res* 36: 149–162, 1997.
16. **Igelmund P, Fleischmann BK, Fischer IR, Soest J, Gryshchenko O, Bohm-Pinger MM, Sauer H, Liu Q, and Hescheler J.** Action potential propagation failures in long-term recordings from embryonic stem cell-derived cardiomyocytes in tissue culture. *Pflügers Arch* 437: 669–679, 1999.
17. **Ji GJ, Fleischmann BK, Bloch W, Feelisch M, Andressen C, Addicks K, and Hescheler J.** Regulation of the L-type Ca²⁺ channel during cardiomyogenesis: switch from NO to adenylyl cyclase-mediated inhibition. *FASEB J* 13: 313–324, 1999.
18. **Johnson CM, Green KG, Kanter EM, Bou-Abboud E, Safitz JE, and Yamada KA.** Voltage-gated Na⁺ channel activity and connexin expression in Cx43-deficient cardiac myocytes. *J Cardiovasc Electrophysiol* 10:1390–401, 1999.
19. **Kamino K.** Optical approaches to ontogeny of electrical activity and related functional organization during early heart development. *Physiol Rev* 71: 53–91, 1991.
20. **Kamino K, Hirota A, and Fujii S.** Localization of pacemaking activity in early embryonic heart monitored using voltage-sensitive dye. *Nature* 290: 595–597, 1981.
21. **Kehat I, Kenyagin-Karsenti D, Snir M, Segev H, Amit M, Gepstein A, Livne E, Binah O, Itskovitz-Eldor J, and Gepstein L.** Human embryonic stem cells can differentiate into myocytes with structural and functional properties of cardiomyocytes. *J Clin Invest* 108: 407–414, 2001.
22. **Liu W, Yasui K, Arai A, Kamiya K, Cheng J, Kodama I, and Toyama J.** β-Adrenergic modulation of L-type Ca²⁺-channel currents in early-stage embryonic mouse heart. *Am J Physiol Heart Circ Physiol* 276: H608–H613, 1999.
23. **Maltsev VA, Ji GJ, Wobus AM, Fleischmann BK, and Hescheler J.** Establishment of beta-adrenergic modulation of L-type Ca²⁺ current in the early stages of cardiomyocyte development. *Circ Res* 84: 136–145, 1999.
24. **Maltsev VA, Rohwedel J, Hescheler J, and Wobus AM.** Embryonic stem cells differentiate in vitro into cardiomyocytes representing sinusnodal, atrial and ventricular cell types. *Mech Dev* 44: 41–50, 1993.
25. **Maltsev VA, Wobus AM, Rohwedel J, Bader M, and Hescheler J.** Cardiomyocytes differentiated in-vitro from embryonic stem cells developmentally express cardiac-specific genes and ionic currents. *Circ Res* 75: 233–244, 1994.
26. **Meyer N, Jaconi M, Landopoulou A, Fort P, and Puceat M.** A fluorescent reporter gene as a marker for ventricular specification in ES-derived cardiac cells. *FEBS Lett* 478: 151–158, 2000.
27. **Metzger JM, Lin WI, and Samuelson LC.** Vital staining of cardiac myocytes during embryonic stem cell cardiogenesis in vitro. *Circ Res* 78: 547–552, 1996.
28. **Miller-Hance WC, LaCorbiere M, Fuller SJ, Evans SM, Lyons G, Schmidt C, Robbins J, and Chien K.** In vitro chamber specification during embryonic stem cell cardiogenesis. *J Biol Chem* 268: 25244–25252, 1993.
29. **Moorman AFM, de Jong F, Denyn MMFJ, and Lamers WH.** Development of the cardiac conduction system. *Circ Res* 82: 629–644, 1998.
30. **Mueller M, Fleischmann BK, Selbert S, Ji GJ, Endl E, Middeler G, Mueller OJ, Schlenke P, Frese S, Wobus AM, Hescheler J, Katus HA, and Franz WM.** Selection of ventricular-like cardiomyocytes from ES cells in vitro. *FASEB J* 14: 2540–2548, 2000.
31. **Nagy A, Rossant J, Nagy R, Abramow-Newerly W, and Roder JC.** Derivation of completely cell culture-derived mice from early-passage embryonic stem cells. *Proc Natl Acad Sci USA* 90: 8424–8428, 1993.
32. **Nuss HB and Marban E.** Electrophysiological properties of neonatal mouse cardiac myocytes in primary culture. *J Physiol* 479: 265–279, 1994.
33. **Oyamada Y, Komatsu K, Kimura H, Mori M, and Oyamada M.** Differential regulation of gap junction protein (connexin) genes during cardiomyocytic differentiation of mouse embryonic stem cells in-vitro. *Exp Cell Res* 229: 318–326, 1996.
34. **Oyamada M, Oyamada Y, Komatsu K, Mori M, and Takamatsu T.** In vitro cardiomyocyte differentiation of mouse embryonic stem cells deficient in gap junction protein connexin 43. *Cardiac Vasc Regen* 1: 54–64, 2000.

35. **Phoon CK, Aristizabal O, and Turnbull DH.** 40 MHz Doppler characterization of umbilical and dorsal aortic blood flow in the early mouse embryo. *Ultrasound Med Biol* 26: 1275–1283, 2000.
36. **Regehr WG, Pine J, Cohan CS, Mischke MD, and Tank DW.** Sealing cultured invertebrate neurons to embedded dish electrodes facilitates long-term stimulation and recording. *J Neurosci Methods* 30: 91–106, 1989.
37. **Robbins J, Gulick J, Sanchez A, Howles P, and Doetschmann T.** Mouse embryonic stem cells express the cardiac myosin heavy chain genes during development in vitro. *J Biol Chem* 265: 11905–11909, 1990.
38. **Satin J, Fujii S, and DeHaan R.** Development of cardiac beat rate in early chick embryos is regulated by regional cues. *Dev Biol* 129: 103–113, 1988.
39. **Spach MS, Barr RC, Serwer GA, Kootsey JM, and Johnson EA.** Extracellular potentials related to intracellular action potentials in dog purkinje system. *Circ Res* 5: 505–519, 1972.
40. **Spach MS, Heidlage JF, Dolber PC, and Barr RC.** Electrophysiological effects of remodeling cardiac gap junctions and cell size. *Circ Res* 86: 302–311, 2000.
41. **Sperelakis N.** Developmental changes in membrane electrical properties of the heart. In: *Physiology and Pathophysiology of the Heart*. Hague, The Netherlands: Nartinus-Nijhoff, 1984, p. 543–573.
42. **Takano M and Noma A.** Development of muscarinic potassium current in fetal and neonatal rat heart. *Am J Physiol Heart Circ Physiol* 272: H1188–H1195, 1997.
43. **Wang L and Duff HJ.** Developmental changes in transient outward current in mouse ventricle. *Circ Res* 81: 120–127, 1997.
44. **Wang L, Feng ZP, Kondo CS, Sheldon RS, and Duff HJ.** Developmental changes in the delayed rectifier K⁺ channels in mouse heart. *Circ Res* 79: 79–85, 1996.
45. **Westfall MV, Pasyk KA, Yule DI, Samuelson LC, and Metzger JM.** Ultrastructure and cell-cell coupling of cardiac myocytes differentiating in embryonic stem cell cultures. *Cell Motil Cytoskeleton* 36: 43–54, 1997.
46. **Wobus AM, Wallukat G, and Hescheler J.** Pluripotent mouse embryonic stem cells are able to differentiate into cardiomyocytes expressing chronotropic responses to adrenergic and cholinergic agents and Ca²⁺ channel blockers. *Differentiation* 48: 173–182, 1991.
47. **Yamamoto M, Honjo H, Niwa R, and Kodama I.** Low-frequency extracellular potentials recorded from the sinoatrial node. *Cardiovasc Res* 39: 360–372, 1998.

